Dimensional topography of the canine frontal sinus as an experimental model of sinus surgery

Han-Seok Kim, D.D.S., M.S.

Department of Dentistry

The Graduate School, Yonsei University

Dimensional topography of the canine frontal sinus as an experimental model of sinus surgery

Directed by Professor Kyung-Seok Hu, D.D.S., Ph.D.

The Doctoral Dissertation
submitted to the Department of Dentistry,
and the Graduate School of Yonsei University
in partial fulfillment of the requirements for the degree of
Doctor of Philosophy

Han-Seok Kim

December
2013

This certifies that the Doctoral Dissertation of Han-Seok Kim is approved.

Thesis Supervisor : **Prof. Kyung-Seok Hu**

Thesis Committee Member : **Prof. Hee-Jin Kim**

Thesis Committee Member : **Prof. Seong-Taek Kim**

Thesis Committee Member : **Prof. Ui-Won Jung**

Thesis Committee Member : **Prof. Sungtae Kim**

The Graduate School
Yonsei University

December 2013

ACKNOWLEDGEMENTS

본 논문이 완성되기까지 시종일관 아낌없는 배려와 세심한 지도를 해주신 김 희진 교수님과 허 경석 교수님께 깊은 감사를 드립니다. 또한 바쁘신 와중에도 많이 지도해 주신 김 성택 교수님, 김 성태 교수님, 정 의원 교수님께도 깊은 감사 말씀 드립니다.

또한 본 연구의 처음부터 이 논문이 나오기까지 지속적으로 궂은 일을 도맡아 하며 자기 일처럼 실험을 도와주신 해부파트 모든 조교 선생님들께도 감사의 마음을 전합니다. 특히 배 정희 선생님과 양 헌무 선생님께 깊이 감사 드립니다.

끝으로, 제가 이 자리에 올 때까지 항상 자식 사랑에 한없는 희생을 하시고 지금까지 키워주신 아버지, 안타깝게도 졸업을 못보시고 돌아가신 어머니, 아낌없는 격려와 끝없는 내조로 제가 학문의 길을 계속해서 정진할 수 있도록 도와준 사랑하는 아내 한 송이, 귀여운 딸, 나현 공주, 아현 공주와 이 작은 결실의 기쁨을 함께 하고 싶습니다.

2013년 12월

저자 씀

TABLE OF CONTENTS

LIST OF FIGURES

LIST OF TABLES

Abstract

Dimensional topography of the canine frontal sinus as an experimental model of sinus surgery

Han-Seok Kim D.D.S., M.S.

Department of Dentistry
The Graduate School, Yonsei University

(Directed by Professor Kyung-Seok Hu D.D.S., Ph.D.)

Sinus floor elevation is implemented widely to overcome unfavorable anatomical conditions on which standard length implants could not be placed. There have been maxillary sinus models in various animals to evaluate the efficacy of surgical interventions. Dogs are widely used as experimental subjects. However, the canine maxillary sinus is difficult to be approached and too small to be manipulated for dental implant placement. The dog frontal sinus may represent an alternative candidate for surgical interventions pertaining to dental implants; its topographical resemblance to the maxillary sinus renders it a potentially favorable experimental environment. The aim of this study was thus to elucidate the anatomical configuration of the canine frontal sinus (e.g., its thickness at different locations) and histological characteristics, and to determine whether it could be a new canine experimental model for dental implant research.

Twenty-four sides of canine frontal bones were harvested from 12 mongrel dogs. The specimens were scanned with a microcomputed tomography system. After three-dimensional reconstruction of the images, the distance from the nasion to the emerging point of the lateral frontal sinus was measured with the aid of Lucion software. The specimens were sectioned in a coronal plane from the emerging point of the lateral aspect of the canine frontal sinus, posteriorly at 1mm intervals, and named coronal sectioned image CS1 (the emerging point of the lateral frontal sinus) to CS16 (the 16th coronal section that was 16mm posterior to CS1). The thicknesses of the canine frontal sinus wall were measured at distances of 3, 6, 9, 12, and 15mm from the midsagittal plane in sections CS1 to CS16. In two of the specimens, the samples were sectioned at a thickness of 7㎛ and stained with hematoxylin and eosin.

The mean distance from the nasion to the emerging point of the lateral frontal sinus was 16.0mm (range, 10.2~23.0mm). The emerging point of the lateral aspect of the canine frontal sinus differed significantly according to the location of the septa within the frontal sinus. The mean thicknesses at 3, 6, 9, 12,and 15mm lateral to the midsagittal plane were 2.3mm (range, 2.0~2.7mm), 2.7mm (range, 2.5~3.4mm), 3.2mm (range, 2.9~3.9mm), 3.8mm (range, 3.1~4.2mm), and 3.7mm (range, 3.2~4.0mm), respectively. There was a tendency toward a greater thickness on proceeding laterally from the midsagittal plane and on proceeding posteriorly from the nasion. The canine frontal sinus was lined with pseudostratified ciliated columnar epithelium comprising cilia and abundant single-layered cells in a manner suggestive of multiple cell layers comprising goblet cells.

The thickest region was from the nasion at 7~8mm and 14~16mm posteriorly, and from the midsagittal plane 12mm laterally (range, 4.0~4.2mm), and from the nasion 6~8mm posteriorly and from the midsagittal plane 15mm laterally (4.0mm). The thinnest region was from the midsagittal plane 3mm laterally (range, 2.1~2.7mm). These data suggest that the canine frontal sinus is a suitable alternative to the canine maxillary sinus as a model for studying various sinus augmentation protocols.

Key words : Sinus augmentation, Frontal Sinus, Dog, Experimental study, Implantation

Dimensional topography of the canine frontal sinus as an experimental model of sinus surgery

Han-Seok Kim, D.D.S., M.S.

Department of Dentistry, The Graduate School,
Yonsei University

(Directed by Professor Kyung-Seok Hu D.D.S., Ph.D.)

I. INTRODUCTION

Dental implant placement has been established as one of the most favorable treatment options for edentulous area. In the early researches about dental implant, the material properties, mechanical features and surface modification of titanium fixtures were investigated (Mayfield et al., 2001; Soncini et al., 2002). Validity of various restorative modalities using dental implants was also studied (Bertin, 1989; Bishop et al., 2007). With improvement in macro and micro design of implant, and development of restorative modalities showing predictable treatment outcomes, did rehabilitation in limited amount of bone or in the situation with poor bone quality become possible. Werbitt and Goldberg (1992) showed that an intact extraction socket is not essential for the successful integration of a titanium implant fixture. Misch et al. (1999) described that ideal treatment plan and implant placement could not be obtained without careful evaluation of mechanical properties of trabecular bone. Improvement in radiographic technology from periapical radiograph to computed tomography (CT) enabled precise treatment plan and implant placement (Gher and Richardson, 1995). Hu et al. (2012) showed implant placement based on treatment plan using CT and planning program was more accurate than panorama radiograph in a cadaver study.

Application of bone substitute and barrier membrane became a valuable treatment modality in clinical cases with bony defects around dental implants. Mayfield et al. (1997) showed that implant success with new bone formation when a bioabsorbable membrane was used in challenging defect around implant. Kim et al. (2011) showed circumferential bone defect (2mm width, 5mm height) around dental implant can be successfully treated with synthetic bone substitute. With the advances in radiographic technologies, macro and micro design of implant fixture, and regenerative techniques using bone substitute and barrier membrane, patients with a resorbed alveolar ridge in which dental implant placement was not possible could be treated with dental implants.

To overcome unfavorable anatomic conditions such as pneumatization of maxillary sinus, alveolar ridge or bony defect around implant, various animal models have been tried (Lee et al., 2007; Brumund et al., 2004; Asai et al., 2002; Bravetti et al., 1998; Hanisch et al., 1997). Haas et al. (1998) examined the value of bovine hydroxyapatite as a grafting material in one-stage sinus lift procedure to better the bony anchorage of implatns using sheep. Shi et al. (2007) evaluated the combination of surgical-grate calcium sulfate and platelet-rich plasma for alveloar ridge preservation prior to implant placement, and the combination resulted in the enhancement of bone regeneration in the early phase of healing. In a study using dogs, Lee et al. (2007) compared the efficiency of two types of bone in the osseointegration of implants and their effect on height of newly formed bone when installed simultaneously with the implant.

However, studies with human subjects are considered more reliable than animal studies due to the clinical relevance and implication. From human cadaver studies, important information with which dental implant can be placed safely was obtained. Kim et al. (2003) described the clinical characteristics of the maxillary sinus wall based on the morphology of the inferior wall of the maxillary sinus in their cadaveric study. From radiographic evaluation, with CT, postoperative evaluation of dental implant as well as preoperative evaluation is possible without any surgical intervention. Even if the radiographic evaluation of implant stability could not be more accurate than any other test such as removal torque test, histological evaluation of bone to implant contact, approximate evaluation of implant stability can be obtained by this radiographic evaluation (M. J. Kim et al., 2006). As mentioned, the most explicit and definite findings can be only obtained by histological evaluation of tissues around dental implant. Harvesting human specimens around dental implant is usually not possible due to ethical issue. Harvesting tissue around dental implant is possible in cadaver studies. However, clinical appraisal are rare in this case. Thus, experiments and observations using animals are needed to provide valuable histological data regarding cellular responses to dental fixtures.

Kim et al. (2003) reported that the human maxillary sinus extends from the first premolar to the second molar area. It was determined that maxillary alveolar bone is resorbed by 0.7 - 1.9mm/year after tooth extraction (Pietrokovski and Massler, 1967). Thus, the vertical dimension of the alveolar bone in the edentulous premolar and molar areas would be restricted by the maxillary sinus. Therefore, redemption of the shrunken alveolar bone by bone augmentation via the sinus is a commonly accepted strategy for retaining sufficient space and stability for implant placement. If there is an animal model which has a structure similar to human maxillary sinus, it will be helpful for clinicians to understand cellular response around implant which is placed after sinus floor elevation. Charateristic bone formation after bone graft in sinus will be understood better with this model. In addition, better understanding anatomical and histological features of maxillary sinus would be possible with this model. Many studies about maxillary sinus for dental implant placement were performed in animals; dog, sheep, rabbit, goat, and monkey (Lee et al., 2007; Brumund et al., 2004; Asai et al., 2002; Bravetti et al., 1998; Hanisch et al., 1997). Sheep, goats, and monkeys are expensive and difficult to be managed for research, whereas animal such as rabbit and dog is relatively inexpensive (Watanabe et al., 1999). In particular, dogs are widely used as experimental subjects in maxillofacial surgery and orthopedic surgery research (Liu et al., 2012).

The similarity of the respiratory epithelia and maxillary sinus membrane between humans and dogs renders the latter as potentially suitable subjects for sinus research (Jung et al., 2006). In addition, the canine model is easy to maintain, durable, relatively resistant to infection, and of an appropriate size for dental implant experiments (Lee et al., 2007). However, the canine maxillary sinus is difficult to be approached and too small to be manipulated for dental implant placement. A possible alternative to the maxillary sinus for research can be the frontal sinus in dogs, since its topographical resemblance to the maxillary sinus would serve as a favorable experimental environment. Few dental implant studies have been performed on the canine frontal sinus. The frontal sinus can be used effectively for dental implant research if detailed anatomical information is available regarding the positional variations in its thickness (Starokha et al., 1990).

The aim of this study was thus to elucidate the anatomical configuration of the canine frontal sinus, and in particular its thickness at various locations and histological characteristics, with a view to establishing its usefulness as a new canine experimental model for dental implant research.

Ⅱ. MATERIALS & METHODS

1. Materials

Twenty-four sides of canine frontal bones were harvested from 12 mongrel dogs (20 - 25kg body weight) for use in the present study. The soft tissues overlying the frontal bone surface were eliminated, and only undamaged specimens were included in the study. One side of the canine frontal sinus was regarded as a specimen, and no distinction was made between right and left specimens.

2. Methods

Morphology of the frontal sinus using micro-CT

The specimens were scanned with a micro CT system (Skyscan 1076, Skyscan, Antwerp, Belgium). A specimen was placed on the holder between the X-ray source and the CCD camera and kept in the field of view; it was then rotated around the vertical axis at intervals of 0.9° for 180°, producing 200 projections. The X-ray beam was projected onto a phosphorus screen, which converted the X-rays into visible light that could be detected by the CCD camera. The collected data were then digitized by a frame grabber and transmitted to a computer running topographic reconstruction software. Serial two dimensional images obtained by micro CT were cross sectional 1968×1968 pixel images. A three dimensional structural image with voxels of size 35㎛ × 35㎛ ×35㎛ was reconstructed from the two dimensional images (with pixels of 35mm × 35mm).

The lateral frontal sinus was used for observation in this study, because the rostral and medial frontal sinuses are too narrow to be used for implant placement. After the reconstruction procedure, the distance from the nasion to the emerging point of the lateral frontal sinus was measured with the aid of Lucion software (version 1.2, CyberMed, Seoul, Korea)(Fig. 1).

The specimens were sectioned in the coronal plane from the emerging point of the lateral aspect of the canine frontal sinus, posteriorly at 1mm intervals, and named coronal sectioned image CS1 (the emerging point of the lateral frontal sinus) to CS16 (the 16th coronal section that was 16mm posterior to CS1)(Fig. 1b). The thickness of the canine frontal sinus wall was measured at distances of 3, 6, 9, 12, and 15mm from the midsagittal plane in images CS1~CS16 using the Lucion software (Fig. 2). The mean and SD values were calculated for each point for all specimens (n=24) using Microsoft Office Excel (Microsoft, Redmond, WA, USA). The values were compared according to their lateral and posterior locations.

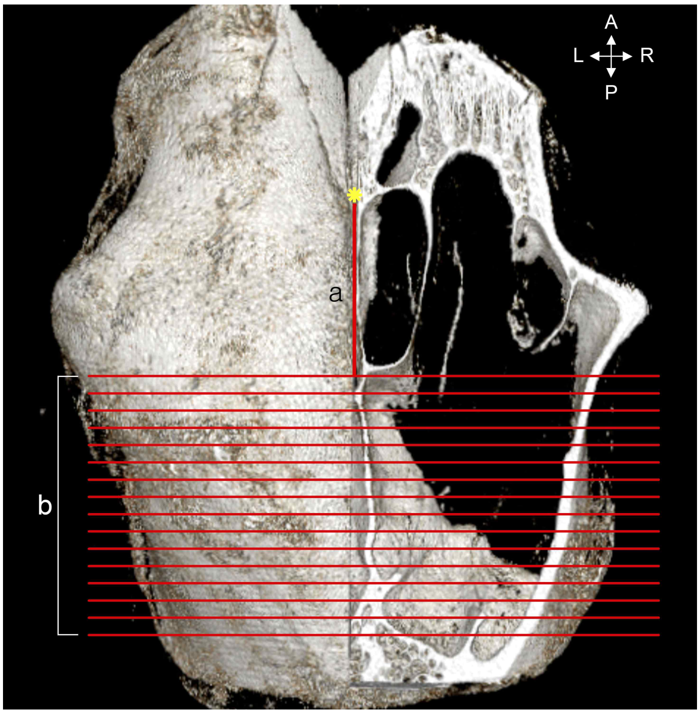

Fig. 1. Parameters measured in the canine frontal bone and sinus with the aid of Lucion software. a, the distance from nasion (yellow asterisk) to the emerging point of the lateral aspect of the canine frontal sinus; b, the 16 coronal sections imaged from the emerging point of the lateral aspect of the canine frontal sinus in the posterior direction at 1mm intervals. A, anterior; P, posterior; L, left; R, right

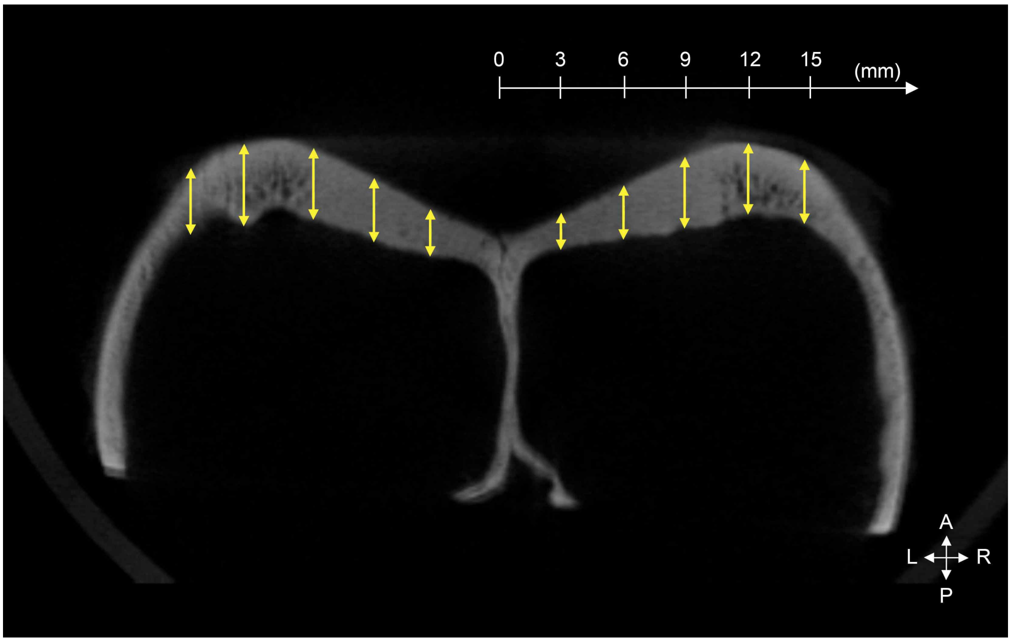

Fig. 2. The thickness of the frontal bone was measured at 3, 6, 9, 12, and 15mm lateral to the midsagittal plane (yellow, double-headed arrows) at 3mm intervals on each coronally sectioned image (CS1~CS16).

Histologic findings

The lateral frontal sinus was decalcified in 10% nitric acid (B96771, Duksan Pure Chemicals, Gyeonggido, Korea) over a period of about 2 weeks. The samples were fixed for 72 hours with 4% paraformaldehyde, embedded in paraffin wax, sectioned at a thickness of 7㎛, and then stained with hematoxylin and eosin. Histological observations were performed with the aid of a light microscope, and photographs were taken using the Leica Microsystem CTR 6000 device (Leica, Wetzlar, Germany).

Ⅲ. RESULTS

1. The distance from the nasion to the emerging point of the lateral frontal sinus

There were septa within the frontal sinus between the nasion and the emerging point of the lateral frontal sinus. The mean distance from the nasion to the emerging point of the lateral frontal sinus was 16.0mm (range, 10.2~23.0 mm)(Fig. 3). The emerging point of the lateral aspect of the canine frontal sinus differed significantly depending on the location of the septa within the frontal sinus.

2. The thickness of the outer table of the frontal bone

The mean thicknesses of the outer table of the canine frontal bone (Table 1) at 3, 6, 9, 12, and 15mm lateral to the midsagittal plane were 2.3mm (range, 2.0~2.7mm), 2.7mm (range, 2.5~3.4mm), 3.2 mm (range 2.9~3.9mm), 3.8mm (range, 3.1~4.2mm), and 3.7mm (range, 3.2~4.0mm), respectively. The mean thickness at 15mm was 1.6 times greater than that at 3mm (Fig. 4).

At 3, 6, and 9mm lateral to the midsagittal plane, the thickness tended to increase slightly from CS1 to CS16. At 12 and 15mm lateral to the midsagittal plane, some differences in thickness were observed from CS1 to CS16. At 12mm, the thickness tended to increase from CS1 to CS8 and from CS11 to CS16, and to decrease from CS8 to CS11. At 15mm, the thickness tended to increase from CS1 to CS8, and to be constant from CS8 to CS16.

The thickest region was from the nasion 7~8 and 14~16mm posteriorly and from the midsagittal plane 12mm laterally (range, 4.0~4.2mm), and from the nasion 6~8mm posteriorly and from the midsagittal plane 15mm laterally (4.0mm). The thinnest region was from the midsagittal plane 3mm laterally (range, 2.1~2.7mm). In general, there was a tendency toward a greater thickness on proceeding laterally from the midsagittal plane and on proceeding posteriorly from the nasion.

Table 1. Mean of the thickness of the frontal bone in dogs

	3mm	6mm	9mm	12mm	15mm
CS 1	2.1 ± 0.4	2.6 ± 0.7	3.0 ± 1.0	3.1 ± 1.0	3.2 ± 0.9
CS 2	2.1 ± 0.5	2.5 ± 0.8	2.9 ± 1.1	3.3 ± 1.1	3.3 ± 1.1
CS 3	2.0 ± 0.4	2.6 ± 0.8	3.0 ± 1.0	3.6 ± 1.3	3.5 ± 1.0
CS 4	2.0 ± 0.5	2.7 ± 0.7	3.1 ± 1.1	3.7 ± 1.3	3.8 ± 1.2
CS 5	2.1 ± 0.6	2.7 ± 0.8	3.1 ± 1.0	3.8 ± 1.3	3.9 ± 1.2
CS 6	2.2 ± 0.6	2.7 ± 0.7	3.3 ± 1.1	3.9 ± 1.3	4.0 ± 1.3
CS 7	2.2 ± 0.6	2.7 ± 0.8	3.3 ± 1.2	4.1 ± 1.3	4.0 ± 1.2
CS 8	2.2 ± 0.6	2.8 ± 0.9	3.5 ± 1.0	4.2 ± 1.3	4.0 ± 1.3
CS 9	2.2 ± 0.8	2.8 ± 0.9	3.4 ± 1.2	3.8 ± 1.1	3.8 ± 1.4
CS 10	2.3 ± 0.8	2.8 ± 1.0	3.6 ± 1.1	3.8 ± 1.2	3.8 ± 1.3
CS 11	2.4 ± 0.9	3.1 ± 0.9	3.6 ± 1.3	3.7 ± 1.2	3.7 ± 1.3
CS 12	2.5 ± 1.0	3.1 ± 1.1	3.7 ± 1.2	3.8 ± 1.3	3.8 ± 1.3
CS 13	2.6 ± 1.0	3.3 ± 1.1	3.7 ± 1.2	3.8 ± 1.3	3.7 ± 1.5
CS 14	2.6 ± 1.1	3.3 ± 1.2	3.8 ± 1.2	4.0 ± 1.4	3.7 ± 1.7
CS 15	2.7 ± 1.0	3.5 ± 1.2	3.9 ± 1.2	4.0 ± 1.5	3.8 ± 1.8
CS 16	2.7 ± 1.0	3.4 ± 1.2	3.9 ± 1.3	4.0 ± 1.6	3.6 ± 1.6

The numbers are mean ± standard deviation. CS1~CS16, the coronal section images from the emerging point of the lateral aspect of the canine frontal sinus to the posterior direction at intervals of 1mm; 3, 6, 9, 12 and 15mm, from the midsagittal plane to lateral direction at intervals of 3mm in each coronal sectioned image.

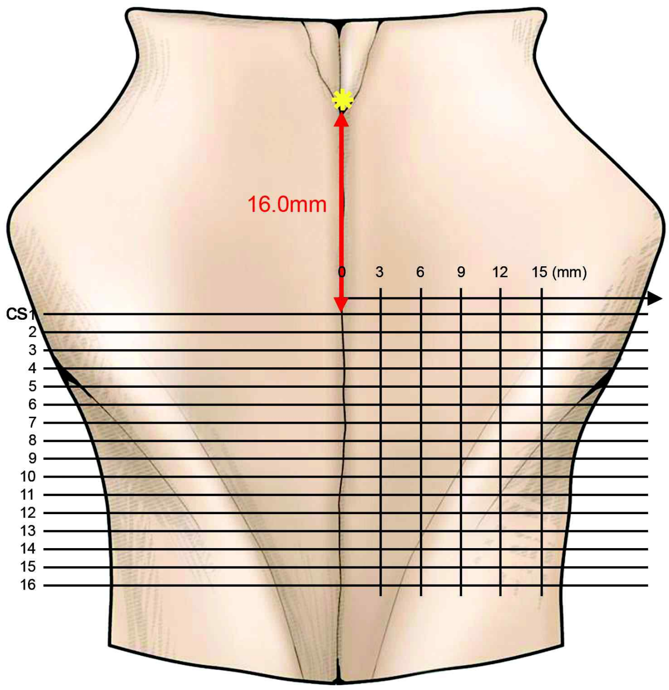

Fig. 3. The distance from the nasion to the emerging point of lateral frontal sinus (red;double headed arrow). *;Nasion

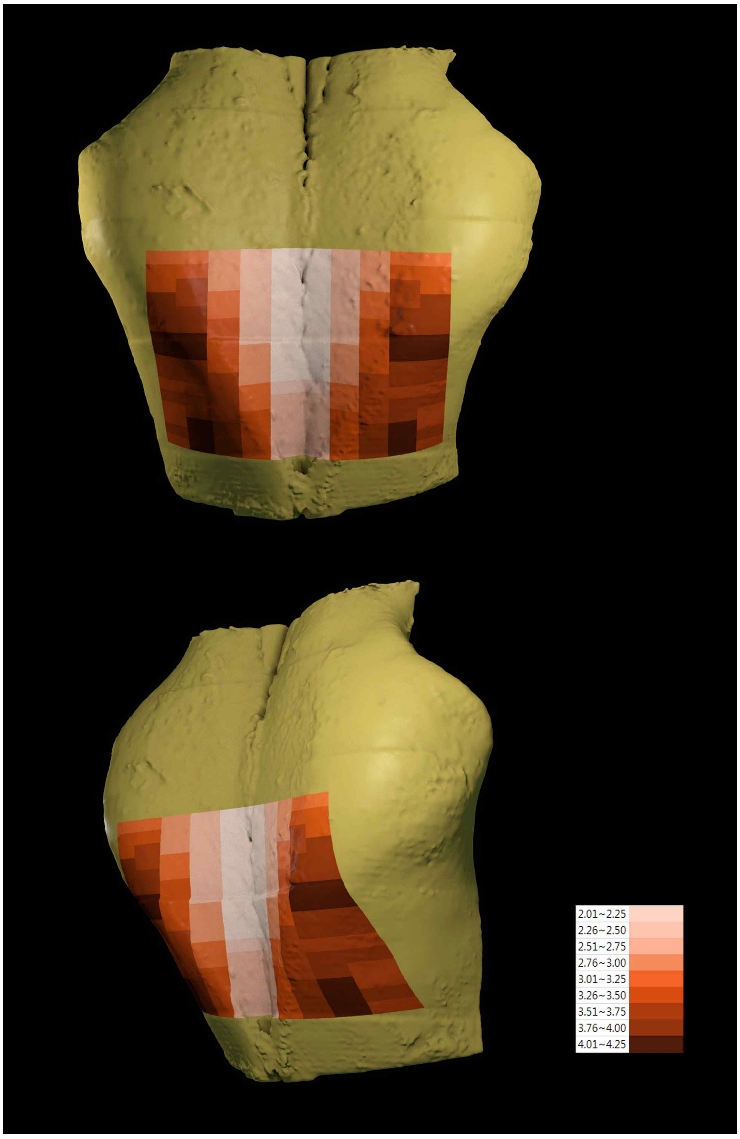

Fig. 4. Topographic thickness of the canine frontal sinus wall (Dorsal aspect). **Measurement**; 3, 6, 9, 12, and 15mm from the midsagittal plane in images CS1~CS16 (unit:mm)

3. Histological findings

The microscopic examination of the internal side of the canine sinus demonstrated that the lining epithelium comprised layers of nonkeratinized epithelium, basement membrane, and lamina propria. Ciliated epithelium was observed lining the internal surface of the sinus (Fig. 5a). There was a distinctly stained line of tight junctions, and the cilia of the outer epithelium were observed on the outside of that line. The eosinophilic cytoplasmic area was located below the tight junction line. A nuclear column typically comprising 5~10 cells was found between the tight junction line and the basement membrane, arranged vertically. Since the nucleus of the outmost cell was squashed horizontally in the stratified epithelium, the nuclear column of the canine sinus lining epithelium was considered as pseudostratified rather than stratified. The epithelial cells overlapped, and the nucleus was superimposed in the image, revealing a vertically stratified arrangement. The lamina propria was observed below the basement membrane, and the vasculature was found among the cells of the lamina propria. Goblet cells were observed among the epithelial cells in higher magnification images (Fig. 5b). Notably, the cilia of the epithelial cells were outside the tight junction line. Microscope images showed that the canine frontal sinus was lined by a pseudostratified ciliated columnar epithelium, comprising cilia and abundant single layered cells in a manner suggestive of multiple cell layers comprising goblet cells.

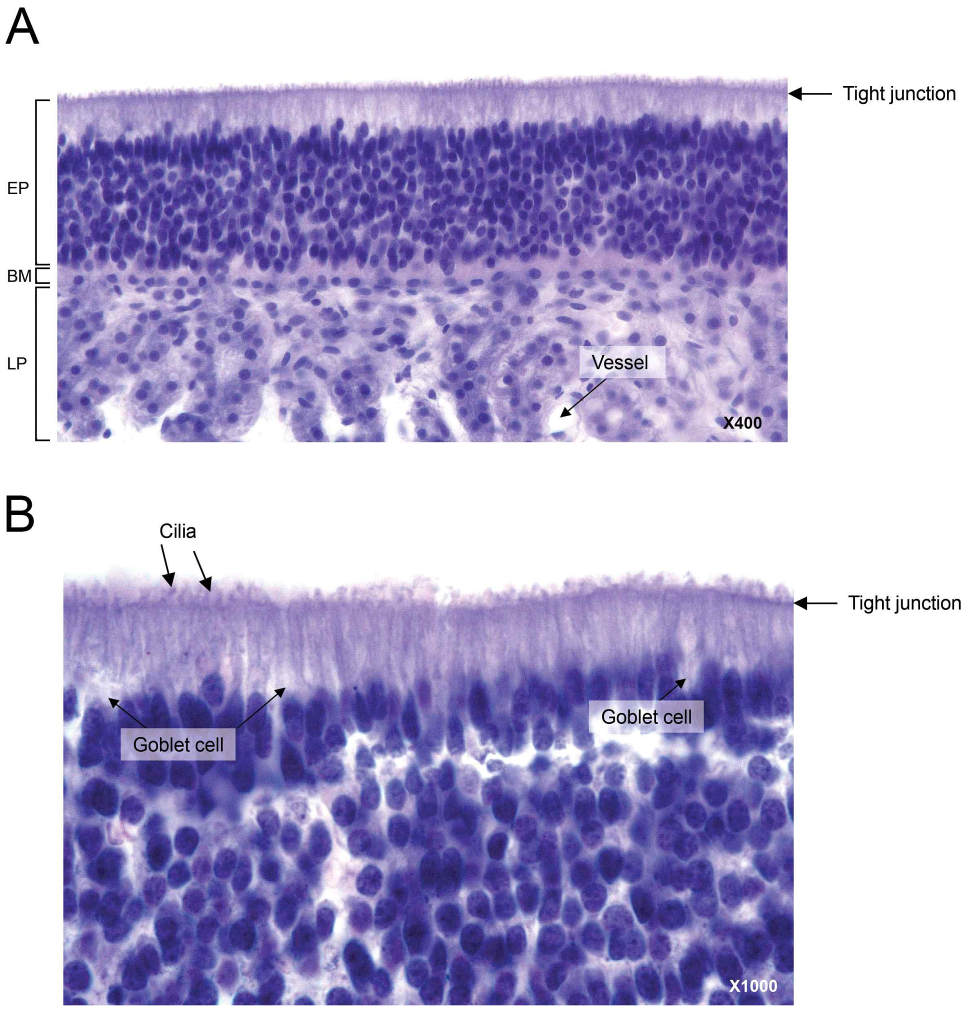

Fig. 5. Histological examination of the canine frontal sinus mucosa. A, X400 magnification image; B, X1000 magnification image; EP, epithelium; BM, basement membrane; LP, lamina propria

Ⅳ. DISCUSSION

The canine frontal sinus comprises the inner and outer tables of the anterior end of the frontal bone and three compartments of air cavities located within these bony tables: the rostral, medial, and lateral frontal sinuses. The lateral frontal sinus, which is the largest of the frontal sinuses, extends into the zygomatic process of the frontal bone (Miller, 1964). In general, animal model should have a proper cortical thickness in the lateral wall, a similar morphology and resistance of the sinus membrane in humans, and an oral approach (Estaca et al., 2008). At based our results, the canine frontal sinus offers several advantages as a model for studying sinus augmentation and its related interventions.

The main advantage of the canine frontal sinus is the extraoral approach which is no necessity for tooth extraction before implantation. Usually, when animal experiment was performed for implantation, the teeth were extracted. After extraction, the healing period was needed for 3~6 months (Jung JH et al., 2006). Bretan et al. (2005) described the method to approach the canine frontal sinus. First, two straight lines were drawn: one along the medial line of the frontal region; and the other at 45° from the pupil. At the intersection point, 1~1.5cm forward and 1cm backward was measured; from these points, an incomplete rectangle delineating the frontal sinus perimeters was drawn. The rectangle area indicates the assumed space of the frontal sinus.

Burrow et al. (2012) reported that the mean depth of the canine frontal sinus was 2.02~2.49cm from the lowest to the deepest points. It thus seems to be sufficiently deep for placement of a regular sized fixture. Furthermore, the approach from the rostral side to the canine frontal sinus facilitates a careful manipulation of bone augmentation involving the sinus and scrupulous placement of the dental fixture. Bilateral placements according to different experimental circumstances can be made on both sides of the canine frontal sinus. Although the effect of mastication on the placed site cannot be examined when using the canine frontal sinus, the stability and histological response of the vital bony tissue can be observed without interference from an uncontrolled oral environment (e.g., microorganisms, hygiene conditions, and eccentric occlusion). Selective investigations of the canine frontal and maxillary sinuses might provide data regarding the relative significance of the oral environment, including mastication, on implant placement, in comparison to a group excluding these factors.

Clinically, one of the more important conditions for successful fixture implantation is the primary stability, the cardinal factor underlying which is the residual bone height. The sinus floor elevation for the primary stability in patients with insufficient bone height is generally approached using one of two methods: (1) the osteotome technique, approaching from the occlusal side of the alveolar ridge, and (2) the window opening procedure, which is performed on the lateral wall of the maxillary sinus (Esfahanizadeh et al., 2012). The osteotome technique has been recommended where there is a residual bone height of at least 6~9mm (Kolerman et al., 2011), while the window opening technique is applied when the residual bone height is lower, at 4~5mm (Del Fabbro et al., 2012). The similarity of the sinus wall thickness between dogs and humans is very important when considering the significance of experimental results obtained with canine subjects relative to the human condition. Thus, the thickness of the canine frontal sinus is very important information with regard to experimental dental implant placement. Nevertheless, few studies have investigated the thickness of the canine frontal sinus; our search of the literature revealed only the study of Toyohiko et al. (2005), which found that the mean thickness of the frontal sinus wall of beagle dogs was 1.24mm at one point. In the present study the mean thicknesses of the lateral frontal sinus wall at 3, 6, 9, 12, and 15mm lateral to the midsagittal plane were 2.3, 2.7, 3.2, 3.8, and 3.7mm, respectively. The mean thickness of the canine frontal sinus wall was lowest at 3mm lateral to the midsagittal plane (2.0~2.2mm). Yang et al. (2009) reported that the mean thickness of the buccofacial wall of the human maxillary sinus was 1.2~1.9mm. Based on these anatomical data, the window opening procedure on the wall canine frontal sinus could be performed with regard to the procedure on the thickest region of human maxillary sinus.

A one stage procedure with immediate loading was previously suggested only for cases with a residual bone height of >4mm (van den Bergh et al., 2000). However, Peleg et al. (2006) reported that the single stage procedure was also suitable for a residual bone height of <4mm with adequate primary stability. Moreover, Fugazzotto and Vlassis (2007) found that placement of a dental implant with immediate loading where there was a residual bone height of 1~4mm was successful in 97.0% of cases. However, further histological analysis of the residual bone height condition of <4mm is needed in animals to establish the efficiency and probability of a successful outcome of immediate loading under these conditions. The mean thickness of the thickest area in this study was 4.0~4.2mm, while that in the other regions of the sinus was <4mm (mean thickness 2.0~3.9mm). Thus, when using the canine frontal sinus model it would be possible to examine the differences in the initial stability of the fixture with immediate loading relative to the bone thickness at multiple sites simultaneously in the same animal.

The maxillary septum acts as a clinical impediment in implant surgery (Beretta et al., 2012). It has been reported that the presence of septa increases the risk of accidental perforation of the maxillary sinus membrane during the sinus lift procedure (Betts and Miloro, 1994; Tatum, 1986; van den Bergh et al., 2000). In the present study, the canine frontal sinus was found to be divided into three regions by septa. The rostral and medial portions of the canine frontal sinus were generally very small and occasionally absent. Thus, the presence of septa was irregular between the nasion and the emerging point of the lateral aspect of the canine frontal sinus. Therefore, this model can be used to experimentally evaluate the effect of the septum at the sinus in the rostral and medial aspects of the canine frontal sinus.

The most common complication during sinus lift surgery is perforation of the maxillary sinus membrane. The mean thickness of the human maxillary sinus membrane has varied widely in previous studies, from 0.1 to 1.0mm (Aimetti et al., 2008; Pommer et al., 2009; Tos and Mogensen, 1979), whereas that of the canine maxillary sinus membrane ranged from 0.6 to 1.4mm (Sul et al., 2008). Although these values did not match exactly, it has been demonstrated that it is possible to perform appropriate implant surgery experiments on the canine maxillary sinus (Choi et al., 2006; Jung et al., 2006; Liu et al., 2012; Sul et al., 2008). Toyohiko et al. (2005) also reported that the canine frontal sinus membrane was intact following implantation into the canine frontal sinus wall.

As with the human maxillary sinus, the canine maxillary sinus is known to contain a respiratory epithelium. The normal dog maxillary sinus mucosa is lined with a pseudostratified epithelium (Choi et al., 2006), and similarly, the epithelial lining of the canine frontal sinus is composed of a pseudostratified ciliated columnar epithelium (PCCE) and goblet cells (Abramson and Eason, 1977). The findings of the present study concur with these previous data; the canine frontal sinus membrane was lined with a PCCE, similar to the human maxillary sinus membrane. The ciliated epithelium acts to transport fluids such as pus and mucus. The canine frontal sinus is also relatively resistant to infection. The similarity of the presence of a lining membrane with a ciliated epithelium in the human and dog sinuses supports the acceptability of the canine frontal sinus as a model for studying implant placement and bone augmentation.

In conclusion, the present study has provided some detailed anatomical data regarding the canine frontal sinus, such as its thickness at different regions, and the characteristics of the sinus mucosa, which are pertinent to dental implant research. Furthermore, the findings show that the canine frontal sinus is a suitable alternative model for studying various parameters of sinus augmentation.

Ⅴ. CONCLUSION

The conclusions of this study are as follows.

1. There were irregular septa within the frontal sinus between the nasion and the emerging point of the lateral aspect of the canine frontal sinus (mean distance, 16mm; range 10.2~23.0mm).

2. The thickness of the sinus wall tended to increase slightly from CS1 to CS16 at 3, 6, and 9mm lateral to the midsagittal plane. The thickness tended to increase from CS1 to CS8 and from CS12 to CS16, and to decrease from CS9 to CS11 at 12mm lateral to the midsagittal plane, and to increase from CS1 to CS8 and decrease from CS9 to CS16 at 15mm lateral to the midsagittal plane.

3. The canine frontal sinus was found to be lined with a PCCE comprising cilia and abundant single layered cells in a manner suggestive of multiple cell layers comprising goblet cells.

4. The present study provides anatomical information about the canine frontal sinus thickness and the characteristics of the sinus mucosa that is relevant to dental implant research.

5. The canine frontal sinus appears to be a suitable alternative to the canine maxillary sinus for experimental and histological studies of various parameters of sinus augmentation.

REFERENCES

Abramson AL, Eason RL: Experimental frontal sinus obliteration: long term results following removal of the mucous membrane lining. Laryngoscope 87: 1066-1073, 1977.

Aimetti M, Massei G, Morra M, Cardesi E, Romano F: Correlation between gingival phenotype and Schneiderian membrane thickness. Int J Oral Maxillofac Implants 23: 1128-1132, 2008.

Asai S, Shimizu Y, Ooya K: Maxillary sinus augmentation model in rabbits: effect of occluded nasal ostium on new bone formation. Clin Oral Implants Res 13: 405-409, 2002.

Beretta M, Cicciu M, Bramanti E, Maiorana C: Schneider membrane elevation in presence of sinus septa: anatomic features and surgical management. Int J Dent 2012: Article ID 261905, 1-6, 2012.

Bertin PM: The use of multiple implant modalities in the management of the edentulous patient. Compendium 10: 657-658, 660-651, 1989.

Betts NJ, Miloro M: Modification of the sinus lift procedure for septa in the maxillary antrum. J Oral Maxillofac Surg 52: 332-333, 1994.

Bishop K, Addy L, Knox J: Modern restorative management of patients with congenitally missing teeth: 4. The role of implants. Dent Update 34: 79-80, 82-84, 2007.

Bravetti P, Membre H, Marchal L, Jankowski R: Histologic changes in the sinus membrane after maxillary sinus augmentation in goats. J Oral Maxillofac Surg 56: 1170-1176; discussion 1177, 1998.

Bretan O, Nogueira EA, Silva EF, Trindade SH: Training the osteoplastic flap technique in dogs. Braz J Otorhinolaryngol 71: 140-144, 2005.

Brumund KT, Graham SM, Beck KC, Hoffman EA, McLennan G: The effect of maxillary sinus antrostomy size on xenon ventilation in the sheep model. Otolaryngol Head Neck Surg 131: 528-533, 2004.

Burrow R, McCarroll D, Baker M, Darby P, McConnell F, Cripps P: Frontal sinus depth at four landmarks in breeds of dog typically affected by sinonasal aspergillosis. Vet Rec 170: 20, 2012.

Choi BH, Zhu SJ, Jung JH, Lee SH, Huh JY: The use of autologous fibrin glue for closing sinus membrane perforations during sinus lifts. Oral Surg. Oral Med. Oral Pathol. Oral Radiol. 101: 150-154, 2006.

Del Fabbro M, Corbella S, Weinstein T, Ceresoli V, Taschieri S: Implant survival rates after osteotome mediated maxillary sinus augmentation: a systematic review. Clin Implant Dent Relat Res 14 Suppl 1: e159-168, 2012.

Esfahanizadeh N, Rokn AR, Paknejad M, Motahari P, Daneshparvar H, Shamshiri A: Comparison of lateral window and osteotome techniques in sinus augmentation: histological and histomorphometric evaluation. J Dent (Tehran) 9: 237-246, 2012.

Estaca E, Cabezas J, Uson J, Sanchez-Margallo F, Morell E, Latorre R: Maxillary sinus-floor elevation: an animal model. Clin Oral Implants Res 19: 1044-1048, 2008.

Fugazzotto PA, Vlassis J: Report of 1633 implants in 814 augmented sinus areas in function for up to 180 months. Implant Dent 16: 369-378, 2007.

Gher ME, Richardson AC: The accuracy of dental radiographic techniques used for evaluation of implant fixture placement. Int J Periodontics Restorative Dent 15: 268-283, 1995.

Haas R, Donath K, Fodinger M, Watzek G: Bovine hydroxyapatite for maxillary sinus grafting: comparative histomorphometric findings in sheep. Clin Oral Implants Res 9: 107-116, 1998.

Hanisch O, Tatakis DN, Rohrer MD, Wohrle PS, Wozney JM, Wikesjo UM: Bone formation and osseointegration stimulated by rhBMP 2 following subantral augmentation procedures in nonhuman primates. Int J Oral Maxillofac Implants 12: 785-792, 1997.

Hidaka toyohiko, Wtanabe takao, Sato junichi: An experimental study on maxillary sinus floor elevation and simultaneous implant placement into the frontal sinus of dogs using bone substitutes. Tsurumi University Dental J 31: 65-80, 2005

Hu KS, Choi DY, Lee WJ, Kim HJ, Jung UW, Kim S: Reliability of two different presurgical preparation methods for implant dentistry based on panoramic radiography and cone-beam computed tomography in cadavers. J Periodontal Implant Sci 42: 39-44, 2012.

Jung JH, Choi BH, Zhu SJ, Lee SH, Huh JY, You TM, Lee HJ, Li J.: The effects of exposing dental implants to the maxillary sinus cavity on sinus complications. Oral Surg. Oral Med. Oral Pathol. Oral

Radiol. 102: 602-605, 2006.

Kim HJ, Yoon HR, Kim KD, Kang MK, Kwak HH, Park HD, Han SH, Park CS.: Personal computer based three dimensional reconstruction and simulation of maxillary sinus. Surg Radiol Anat 24: 393-399, 2003.

Kim MJ, Jung UW, Kim CS, Kim KD, Choi SH, Kim CK, Cho KS.: Maxillary sinus septa: prevalence, height, location, and morphology. A reformatted computed tomography scan analysis. J Periodontol 77: 903-908, 2006.

Kim S, Jung UW, Lee YK, Choi SH: Effects of biphasic calcium phosphate bone substitute on circumferential bone defects around dental implants in dogs. Int J Oral Maxillofac Implants 26: 265-273, 2011.

Kolerman R, Moses O, Artzi Z, Barnea E, Tal H: Maxillary sinus augmentation by the crestal core elevation technique. J Periodontol 82: 41-51, 2011.

Lee SH, Choi BH, Li J, Jeong SM, Kim HS, Ko CY: Comparison of corticocancellous block and particulate bone grafts in maxillary sinus floor augmentation for bone healing around dental implants. Oral Surg. Oral Med. Oral Pathol. Oral Radiol. 104: 324-328, 2007.

Liu N, Sun F, Xu C, Lin T, Lu E: A comparative study of dog models for osteotome sinus floor elevation and dental implants in posterior maxilla subjacent to the maxillary sinus. OR SURG OR MED OR PA, 115: e15-20, 2012.

Mayfield L, Nobreus N, Attstrom R, Linde A: Guided bone regeneration in dental implant treatment using a bioabsorbable membrane. Clin Oral Implants Res 8: 10-17, 1997.

Mayfield LJ, Skoglund A, Hising P, Lang NP, Attstrom R: Evaluation following functional loading of titanium fixtures placed in ridges augmented by deproteinized bone mineral. A human case study. Clin Oral Implants Res 12: 508-514, 2001.

Miller ME: Anatomy of the dog, 1st Ed. Saunders, Philadelphia, p190-191, 1964

Misch CE, Qu Z, Bidez MW: Mechanical properties of trabecular bone in the human mandible: implications for dental implant treatment planning and surgical placement. J Oral Maxillofac Surg 57: 700 706; discussion 706-708, 1999.

Peleg M, Garg AK, Mazor Z: Predictability of simultaneous implant placement in the severely atrophic posterior maxilla: A 9 year longitudinal experience study of 2132 implants placed into 731 human sinus grafts. Int J Oral Maxillofac Implants 21: 94-102, 2006.

Pietrokovski J, Massler M: Alveolar ridge resorption following tooth extraction. J Prosthet Dent 17: 21-27, 1967.

Pommer B, Unger E, Suto D, Hack N, Watzek G: Mechanical properties of the Schneiderian membrane in vitro. Clin Oral Implants Res 20: 633-637, 2009.

Shi B, Zhou Y, Wang YN, Cheng XR: Alveolar ridge preservation prior to implant placement with surgical-grade calcium sulfate and platelet-rich plasma: a pilot study in a canine model. Int J Oral

Maxillofac Implants 22: 656-665, 2007.

Soncini M, Rodriguez y Baena R, Pietrabissa R, Quaglini V, Rizzo S, Zaffe D: Experimental procedure for the evaluation of the mechanical properties of the bone surrounding dental implants. Biomaterials 23: 9-17, 2002.

Starokha AV, Itin VI, Kovrizhnykh VV, Ryzhov AI, Monasevich LA: Use of porous permeable titanium nickelide implants in surgery of the frontal and maxillary sinuses (a clinical experimental study). Vestn Otorinolaringol: 64-68, 1990.

Sul SH, Choi BH, Li J, Jeong SM, Xuan F: Histologic changes in the maxillary sinus membrane after sinus membrane elevation and the simultaneous insertion of dental implants without the use of grafting materials. Oral Surg. Oral Med. Oral Pathol. Oral Radiol. 105: e1-5, 2008.

Tatum H, Jr.: Maxillary and sinus implant reconstructions. Dent Clin North Am 30: 207-229, 1986.

Tos M, Mogensen C: Mucus production in the nasal sinuses. Acta Otolaryngol Suppl 360: 131-134, 1979.

van den Bergh JP, ten Bruggenkate CM, Disch FJ, Tuinzing DB: Anatomical aspects of sinus floor elevations. Clin Oral Implants Res 11: 256-265, 2000.

Watanabe K, Niimi A, Ueda M: Autogenous bone grafts in the rabbit maxillary sinus. Oral Surg. Oral Med. Oral Pathol. Oral Radiol. 88: 26-32, 1999.

Werbitt MJ, Goldberg PV: The immediate implant: bone preservation and bone regeneration. Int J Periodontics Restorative Dent 12: 206-217, 1992.

Yang HM, Bae HE, Won SY, Hu KS, Song WC, Paik DJ, Kim HJ.: The buccofacial wall of maxillary sinus: an anatomical consideration for sinus augmentation. Clin Implant Dent Relat Res 11 Suppl 1: e2-6, 2009.

Abstract (in korean)

개의 이마굴을 이용한 새로운 임플란트 실험모델 제시

<지도교수 허 경 석>

연세대학교 대학원 치의학과

김 한 석

위턱뼈 임플란트 식립시 뼈의 흡수가 진행되어 잔존뼈량이 적은 경우에는 위턱굴올림술 (sinus augmentation), 뼈이식술 (bone graft)등을 시행하게 된다. 이와 관련된 전임상 연구들이 많이 시행되고 있으며, 사람과 유사한 크기와 구조를 가지고 있는 개의 위턱굴을 주로 이용하고 있다. 그러나, 개의 위턱굴을 이용할 경우, 접근성의 어려움, 발치에 따른 윤리적인 문제, 발치 후 치유기간이 필요하다는 문제점 등을 가지고 있다. 개는 위턱굴 이외에 3개의 이마굴이 존재하는데 위치에 따라서 각각 앞쪽, 안쪽, 가쪽이마굴이라고 한다. 이들 중에서 가쪽이마굴이 가장 크며, 이마뼈 광대돌기 속을 채우고 뒤쪽으로 확장되어 있다. 따라서, 임플란트 전임상실험을 위하여 위턱굴 대신 이마굴을 이용할 경우 여러가지 문제점들을 해결할 수 있게 된다. 따라서 본 연구는 개의 이마굴의 점막염색과 가쪽이마굴의 뼈 두께 계측을 통하여 임플란트 전임상연구를 위한 새로운 실험모델을 제시하고자 한다.

재료로는 mongrel 24쪽 (20~30kg)을 좌, 우 구분 없이 사용하였다. Micro-CT를 이용하여 이마굴을 촬영한 후, Lucion Software를 이용하여 3차원 재구성하였다. 앞쪽이마굴의 크기는 작았고, 안쪽이마굴은 크기가 작을 뿐만 아니라 없는 경우도 있어 가쪽이마굴만을 이용하였다. 따라서 가쪽이마굴이 시작되는 지점부터 뒤통수뼈 방향으로 16mm까지 1mm간격으로 모두 16개의 관상단면 이미지를 만들었다. 각각의 이미지에서 정중시상면 (midsaggital plane)을 기준으로 가쪽으로 3mm 간격마다 (3mm, 6mm, 9mm, 12mm, 15mm) 두께를 계측하였다. 2쪽의 표본에서 개

이마굴점막을 H/E염색하였다.

코뿌리점에서 가쪽이마굴이 시작되는 지점까지의 거리는 평균 16.0mm (10.2~23.0mm)였으며, 안쪽과 가쪽이마굴 사이에 존재하는 중격의 위치에 따라서 시작되는 지점의 변위차가 컸다. 이마굴의 뼈두께는 정중시상면으로부터 3mm지점의 두께는 2.3mm (2.0~2.7mm)이고, 6mm지점의 두께는 2.7mm (2.5~3.4mm), 9mm지점의 두께는 3.2mm (2.9~3.9mm)이고, 12mm지점의 두께는 3.8mm(3.1~4.2mm), 15mm지점의 두께는 3.7mm (3.2~4.0mm)였으며, 가쪽으로 진행할수록 두꺼워지는 양상을 보였다. 또한, 관상단면을 기준으로 뒤통수뼈 방향으로 1mm단위로 이마굴의 뼈두께 양상을 분석한 결과, 뒤통수뼈 방향으로 갈수록 뼈두께가 점차 두꺼워지는 양상을 보였다. 또한 이마굴 점막은 H/E 염색한 결과 거짓중층원주섬모상피 (PCCE)로 관찰되어으며, 뚜렷한 섬모상피와 술잔세포들이 존재하였다.

결론적으로, 이마굴의 가장 두꺼운 부위는 12mm지점에서는 코뿌리점에서 뒤통수뼈 방향으로 7~8mm 그리고 14~16mm였다. 그리고 15mm지점에서는 코뿌리점에서 뒤통수뼈방향으로 6~8mm 였다. 가장 얇은 부위는 정중시상면에서 가쪽방향으로 3mm지점이었다. 다음과 같은 결과를 토대로 위턱굴올림술과 관련한 다양한 동물실험이 개의 위턱굴뿐만 아니라 이마굴에서도 적절하게 사용될 수 있을것으로 사료된다.

핵심되는 말 : 위턱굴올림술, 개이마굴, 개, 실험연구, 치과임플란트